CONF-970607--6

APPLYING X-RAY DIGITAL IMAGING TO THE VERIFICATION OF CADMIUM IN FUEL-STORAGE COMPONENTS

R. D. Dabbs & D. H. Cook
Oak Ridge National Laboratory
Oak Ridge, Tennessee

Paper to be presented at

1997 Advanced Reactor Safety Meeting
American Nuclear Society
June 1 - June 4, 1997
Orlando, Florida

Prepared by the
Research Reactors Division
OAK RIDGE NATIONAL LABORATORY
Oak Ridge, Tennessee 37831
managed by
LOCKHEED MARTIN ENERGY RESEARCH, CORP.
for the
U.S. DEPARTMENT OF ENERGY
under contract DE-AC05-96OR22464

HH

APPLYING X-RAY DIGITAL IMAGING TO THE VERIFICATION OF CADMIUM IN FUEL-STORAGE COMPONENTS

R. D. Dabbs
Oak Ridge National Laboratory
Post Office Box 2008
Oak Ridge, Tennessee 37831-6392
(423) 576-5582

D. H. Cook
Oak Ridge National Laboratory
Post Office Box 2008
Oak Ridge, Tennessee 37831-6399
(423) 574-5690

ABSTRACT

The High Flux Isotope Reactor utilizes large underwater fuel-storage arrays to stage irradiated fuel before it is shipped from the facility. Cadmium is required as a thermal neutron absorber in these fuel-storage arrays to produce an acceptable margin of nuclear subcriticality during both normal and off-normal operating conditions. Due to incomplete documentation from the time of their fabrication (as early as the mid 1960s), the presence of cadmium within two stainless-steel parts of fuel-storage components (shroud assemblies) removed from old fuel-storage arrays must be experimentally verified before they are reused in new fuel-storage arrays.

A cadmium-verification program has been developed in association with the Waste Examination and Assay Facility located at the Oak Ridge National Laboratory to nondestructively examine these older shroud assemblies. The program includes the following elements (1) x-ray analog imaging, (2) x-ray digital imaging, (3) prompt-gamma-ray spectroscopy measurements, and (4) neutron-transmission measurements. Combining the results of these four program elements provides a high assurance that cadmium is both present and remains in its design configuration.

X-ray digital imaging utilizes an analog-to-digital convertor to record attenuated x-ray intensities observed on a florescent detector by a video camera. These x-ray intensities are utilized in expressions for cadmium thickness based upon x-ray attenuation theory. The thickness expressions require known x-ray attenuation coefficients, x-ray intensities obtained from both the tested shroud assembly and shroud assemblies (standards) of known construction, and other geometrical parameters. X-ray digital imaging has been applied to successfully estimate the cadmium thicknesses in several older shroud assemblies with no damage to them.

I. INTRODUCTION

The continued operation of many research reactors depends on the successful disposition of increasing amounts of irradiated fuel. Although such disposition must eventually include both short-term and long-term storage options (including on-site dry storage, off-site dry storage, reprocessing, etc.), most research-reactor irradiated fuel currently remains stored in water-filled pools. Since this short-term storage option typically involves fuel directly exposed to the pool water, it represents a thermal neutronic system that is both moderated and reflected by full-density water.

A. Background

Research reactors, such as the High Flux Isotope Reactor (HFIR) [1] at the Oak Ridge National Laboratory (ORNL), have both short fuel cycles and limited-size fuel-handling pools. These two factors (combined with limited shipping capability) necessitate the handling and storage of increasingly large quantities of irradiated fuel in water-filled pools. Because most of the parameters available to control the nuclear reactivity (e.g., interaction, moderation, reflection, etc.) of such thermal systems do not provide a sufficient margin of subcriticality, the use of a thermal neutron absorber is required. [2]

Historically (since the mid 1960s), cadmium has been used at the HFIR in stationary fuel-storage components known as shroud assemblies. As shown in Figure 1, each shroud assembly [3] is capable of holding one HFIR core. By design, each shroud assembly was fabricated to contain cadmium sealed within both a double-walled stainless-steel post and a double-walled stainless-steel outer cylinder. Multiple shroud assemblies were mounted on aluminum frames [4] and configured to form low-density (single-tier, horizontally rectangular pitch) fuel-storage arrays (FSAs). Because the cadmium-containing shroud assemblies remained stationary during use, fuel movement into/from them was complicated by requiring the handling of individual fuel elements (two fuel elements comprise a complete HFIR core) to maintain sufficient nuclear subcriticality.

In order to increase the fuel-storage capacity within the HFIR pool, new high-density (multitier, horizontally triangular pitch) FSAs have been designed to replace the old FSAs. [5] The fabrication and installation of these new FSAs is currently on going. Fuel is stored within the high-density FSAs using movable fuel-storage components known as jacket assemblies. [6] As shown in Figure 2, a jacket assembly is similar in design (radial geometry) to a shroud assembly. This similarity allows shroud assemblies, which have been recovered from disassembled low-density FSAs, to be physically converted into jacket assemblies for subsequent use in the high-density FSAs. Because the jacket-assembly design allows cadmium to be integrally moved with fuel, an entire HFIR core can be handled at one time when residing within a jacket assembly.

B. Objective

A cadmium-verification program has been developed in association with the Waste Examination and Assay Facility [7] located at the ORNL to nondestructively examine older shroud assemblies (and new shroud assemblies and jacket assemblies, as required). This program includes the following elements (1) x-ray analog imaging to ensure that the material residing within both the post and outer cylinder remains properly distributed, (2) x-ray digital imaging to ensure that the material residing within the post and outer cylinder is sufficiently thick to be black to thermal neutrons, (3) neutron-transmission and prompt-gamma-ray spectroscopy measurements to ensure that the material residing within the outer cylinder is a strong thermal-neutron absorber and has a cadmium signature, and (4) neutron-transmission measurements to ensure that the material residing within the post is a strong thermal-neutron absorber. This nondestructive verification both compliments the cadmium verification performed during the initial fabrication process (i.e., chemical analysis of its purity, measurement of both its weight and thickness, and witnessing its installation) and is part of the FSA in-service-inspection program.

This paper focuses on the x-ray digital imaging element of the cadmium-verification program. The x-ray analog imaging, which involves real-time recordings of attenuated x-ray intensities as a shroud assembly is rotated, allows a visual verification that the cadmium located within its post and outer cylinder continues to be both uniform and in the as-built configurations. Both the neutron-transmission and the prompt-gamma-ray-spectroscopy measurements are documented elsewhere. [7]

C. Shroud-Assembly Geometry

Only shroud assemblies built prior to January 1991 currently require verification of the presence of cadmium in their posts and outer cylinders before they are reused in the new FSAs. Shroud assemblies (and jacket assemblies) built after that date (1) have fabrication records that adequately verify that cadmium was properly installed and (2) have short service lifetimes compared to the older shroud assemblies being processed through the cadmium verification program.

Three generations of shroud assemblies exist. Shroud assemblies SA-01 through SA-36 represent those fabricated prior to January 1991. Important radial dimensions for this set of shroud assemblies include (1) for the post, a 58-mil thick layer of cadmium residing between the inner (2,063-mil outer radius and 109-mil thickness) and outer (2,250-mil outer radius and 109-mil thickness) stainless-steel walls and (2) for the outer cylinder, a 36-mil thick layer of cadmium residing between the inner (8,813-mil outer radius and 125-mil thickness) and outer (8,911-mil outer radius and 62-mil thickness) stainless-steel walls. The remaining shroud assemblies differ from the first generation in that (1) SA-37 through SA-60 have a thicker post inner (150-mil thickness) and outer (150-mil thickness) wall and a thinner outer-cylinder inner (120-mil thickness) and outer (60-mil thickness) wall and (2) SA-61 through SA-80 have a thinner post-cadmium thickness (36 mils). Jacket assemblies have radial geometries similar to the last generation of shroud assemblies.

II. THEORETICAL BASIS

The attenuation of x-rays through a single medium may be used to calculate the x-ray attenuation coefficients of both stainless steel and cadmium at a given incident x-ray energy. This requires measuring two x-ray intensities resulting from the attenuation of x-rays through two known thicknesses of each material. The variances of the measured x-ray attenuation coefficients may then be determined using standard error propagation. Once the x-ray attenuation coefficients for stainless steel and cadmium are known, the attenuation of x-rays along a known path through a shroud assembly may be used to estimate the internal cadmium thicknesses.

Given a source of uncharged particles experiencing simple absorption in a media (with no secondary or scattering radiation), the relationship between the incident (I_o) and exit (I) x-ray intensities may be written as

$$I = I_o \, e^{-\mu z} \tag{1}$$

where μ is the x-ray attenuation coefficient of the media and z is the length of the known x-ray path. Equation 1 may be written for two known material thicknesses so that

$$I_o = \frac{I_1}{e^{-\mu z_1}} = \frac{I_2}{e^{-\mu z_2}} \tag{2}$$

where z_1 represents the first known material thickness and z_2 represents the second known material thickness.

A. Attenuation Coefficients

As evidenced by the shroud-assembly radial geometry, an x-ray that completely penetrates its diameter must traverse through several stainless-steel and cadmium layers. Because the attenuation of x-rays through these materials depends on their x-ray attenuation coefficients (dependent on the energy of the incident x-ray), these coefficients are experimentally determined as part of each shroud-assembly verification using calibration plates (either stainless steel or cadmium) of known thicknesses. Solving Equation (2) for μ yields

$$\frac{I_1}{I_2} = \frac{e^{-\mu z_1}}{e^{-\mu z_2}} = e^{-\mu z_1 - (-\mu z_2)} \tag{3}$$

$$\mu = \ln\left(I_1 / I_2\right) / \left(z_2 - z_1 \right)$$

which may be used to calculate the x-ray attenuation coefficient (for a given incident x-ray energy) by knowing the average x-ray intensities at the detector (I_1 and I_2) and the calibration-plate thicknesses (z_1 and z_2).

B. Attenuation-Coefficient Uncertainty

Assuming no correlation between state variables, the variance of μ may be estimated by

$$\sigma_\mu^{\,2} = \sum_{i=1}^{n} \left(\frac{\partial \mu}{\partial q_i} \right)^2 \sigma_{q_i}^{\,2} \tag{4}$$

where n equals 4, q_1 is I_1, q_2 is I_2, q_3 is z_1, q_4 is z_2, and the partial derivatives are obtained from Equation 3. Because the intensities are recorded using an analog-to-digital convertor providing 256 shades of gray, the variance of each digitized x-ray intensity is represented as a combination of the variance of the digitized data (classical histogram variance) and the variance of the digitization process, which involves both the standard pixel error and the mean dynamic range of the analog-to-digital convertor. The variances of the known thicknesses are obtained directly from thickness measurements performed on the calibration plates.

C. Cadmium Thickness

Equation 2 may be written for a multilayered shroud assembly to be verrified and a comparative standard shroud assembly (having [9] known geometry and cadmium content) as

$$I_o = \frac{I_{vfd}}{e^{-\sum_{i=1}^{n} \mu_{i,vfd} \, z_{i,vfd}}} = \frac{I_{std}}{e^{-\sum_{i=1}^{m} \mu_{i,std} \, z_{i,std}}} \tag{5}$$

where *vfd* indicates parameters related to the shroud assembly being verified, *std* indicates parameters related to a standard shroud assembly having a known composition, n equals the number of layers of the shroud assembly being verified along which the x-ray path extends, and m equals the number of layers of the shroud assembly having a known composition along which the x-ray path extends.

Equation 5 may be used to determine the total cadmium thickness through which the x-rays traverse. For the outer-cylinder path, this thickness involves two cadmium layers; whereas, for the post path, this thickness involves four cadmium layers. Solving for z_{cd},

$$z_{cd,vfd} = \left[\ln\left(I_{std} / I_{vfd} \right) / \mu_{cd} + \mu_{ss} \left(z_{ss,std} - z_{ss,vfd} \right) / \mu_{cd} + z_{cd,std} \right] \tag{6}$$

where the two x-ray attenuation coefficients have been previously determined and the three thicknesses are known from as-built data.

D. Cadmium-Thickness Uncertainty

Assuming no correlation between system variables, the variance of z_{cd} may be estimated by

$$\sigma_{z_{cd,vfd}}^{\,2} = \sum_{i=1}^{n} \left(\frac{\partial z_{cd,vfd}}{\partial q_i} \right)^2 \sigma_{q_i}^{\,2} \tag{7}$$

where n equals 4, q_1 is I_{std}, q_2 is I_{vfd}, q_3 is μ_{ss}, q_4 is μ_{cd}, and the partial derivatives are obtained from Equation 6. As before, the variance of each digitized x-ray intensity is represented as a combination of the variance of the digitized data and the variance of the digitization process. The variances of the x-ray attenuation coefficients are determined from Equation 4. No uncertainty is applied to $z_{ss,\,std}$, $z_{cd,\,std}$, and $z_{ss,\,vfd}$ in Equation 7.

E. Digital-Imaging Processing

The resolution of the image-recording system provides a digitized image of detector x-ray intensity that is circular in shape with a radius of over 200 pixels. Because of halo effects occurring in the fringe of each digitized image, only its center portion is utilized. This uniform area is represented by a square having 60 pixels on a side. The circle circumscribing such a square has a radius of about 40 pixels (significantly smaller than the fringe radius of about 150 pixels). To address the possible effect of part curvature on the average intensity of each digitized image, the 60x60 square is further subdivided into three equal segments having a width (horizontal) of 20 pixels and a height (vertical) of 60 pixels. Averages are then determined using histograms of the following eight pixel sets: the overall 60x60 square, the three 20x60 rectangular thirds of the square, and the four 1x60 lines representing the two square vertical sides and the two lines subdividing the square into thirds. No significant variations in the averages of these eight pixel sets indicates no significant influence of part curvature on the average intensity of a digitized image.

III. EXPERIMENTAL SETUP

Referring to Figure 1, the radial geometry (at an elevation within the cadmium domain) of a typical HFIR shroud assembly consists of a double-walled stainless-steel post having an internal layer of cadmium and a double-walled stainless-steel outer cylinder having an internal layer of cadmium. Digital x-ray imaging is performed by passing x-rays horizontally through a stationary shroud assembly along the two paths shown in Figure 3. Because the x-ray source and detector (a fluorescent screen observed by a charge-coupled device video camera) both reside externally to the shroud assembly, the outer-cylinder (annulus) x-ray path must penetrate six material layers (four stainless steel and two cadmium) and the post x-ray path must penetrate twelve material layers (eight stainless steel and four cadmium). As indicated in Figure 3 by the patterned areas, the curvature of the post and outer cylinder may be significant over the width of the acquisition area of the image (about 6 by 6 inches).

The stainless-steel and cadmium x-ray attenuation coefficients are measured as shown in Figure 4. A set of flat calibration plates (having a desired total thickness) are positioned between the x-ray source and detector. Digital x-ray imaging is performed by passing x-rays horizontally through these stationary plates. Detector intensities are measured for several incident x-ray energies and total plate thicknesses for each of the two materials. The lead shield minimizes x-ray leakage around the calibration plates.

IV. RESULTS

To date, x-ray digital imaging has been performed on several shroud assemblies. Each of these shroud assemblies has been shown to contain cadmium both in its post and outer cylinder of sufficient thickness (greater than about 10 mils) [8] to be black to thermal neutrons. The following methodology was used to calculate cadmium thicknesses in each of these shroud assemblies.

The x-ray attenuation coefficients (with variances) of cadmium and stainless steel are first determined using Equations 3 and 4 and the experimental setup shown in Figure 4. For each material, six digital images are captured (using three material thicknesses and two incident x-ray energies). For each incident x-ray energy, three x-ray attenuation coefficients (with variances) are determined and subsequently averaged (with combined variance). For conservatism (to provide thinner calculated cadmium thicknesses from Equation 6), the cadmium and stainless-steel x-ray attenuation coefficients are increased and decreased by 10 percent, respectively.

For both the annular (outer-cylinder) and post paths, the total cadmium thickness (with variance) of the shroud assembly (i.e., two layers for the outer-cylinder path and four layers for the post path) is determined using Equations 6 and 7 and the experimental setup shown in Figure 3. Four sets of x-ray attenuated intensities are recorded at three incident x-ray energies: (1) annular path for the standard shroud assembly, (2) annular path for the shroud assembly being verified, (3) post path for the standard shroud assembly, and (4) post path for the shroud assembly being verified. For the annular path, the minimum calculated cadmium total thickness is reduced by two standard deviations and divided by two to yield an estimate of the single-layer cadmium thickness. For the post path, the minimum calculated cadmium total thickness is reduced by two standard deviations, reduced by twice the previously calculated outer-cylinder cadmium thickness, and divided by two to yield an estimate of the single-layer cadmium thickness.

Applying the above methodology to shroud assembly SA-28 [9] yielded average cadmium x-ray attenuation coefficients of 0.0087 ± 0.0020 mils^{-1} (incident x-ray energy of 175 kV) and 0.0034 ± 0.0016 mils^{-1} (incident x-ray energy of 225 kV) and average stainless-steel x-ray attenuation coefficients of 0.0032 ± 0.0006 mils^{-1} (incident x-ray energy of 175 kV) and 0.0013 ± 0.0007 mils^{-1} (incident x-ray energy of 225 kV). For the outer-cylinder path, the total calculated minimum cadmium thickness was 86.2 ± 2.7 mils and the single-layer calculated cadmium thickness was 40 mils, which compares well with the nominal cadmium thickness of 36 mils indicated on the as-built drawings. For the post path, the total calculated minimum cadmium thickness was 205.3 ± 15.1 mils and the single-layer calculated cadmium thickness was 47 mils, which compares well with the nominal cadmium thickness of 58 mils indicated on the as-built drawings. Because both of these thicknesses remain significantly above the minimum allowable thickness of 10 mils, the shroud assembly was declared fit for use from the x-ray digital imaging perspective.

V. CONCLUSIONS

The use of cadmium in the HFIR FSAs provides two major fuel-management benefits. First, the capacity of the high-density FSAs is significantly increased. This allows the continued operation of the reactor without either enlarging the existing pools or completing off-site fuel shipments. Second, fuel management is significantly simplified by moving entire HFIR cores at one time. This reduces the number of operations required for each HFIR-core move by a factor of three. The cadmium-verification program, which (1) ensures that the cadmium-containing shroud/jacket assemblies incorporated into the FSAs continue to perform their design functions (even with extended service histories) and (2) allows significant cost savings (from both fabrication and waste-disposal perspectives) to be realized by reusing existing shroud assemblies, provides continued assurance that the FSAs at HFIR remain safely subcritical while helping to control their cost.

ACKNOWLEDGMENTS

The authors thank Dr. K.W. Tobin and Dr. J.A. Chapman of the Oak Ridge National Laboratory for their support of this work.

REFERENCES

1. H. A. Glovier, et al., *High Flux Isotope Reactor Safety Analysis Report,* ORNL/M-2344 (October 1992).

2. R. D. Dabbs, *HFIR Fuel-Storage-Array Criticality Safety Analysis (Multitier)* , C-HFIR-93-058, HFIR Calculation (April 1994).

3. HFIR Drawing, *Shroud Assembly (Assembly),* M-11462-OH-390-E (December 1993)

4. HFIR Drawing, *Four-Seat-Fuel-Storage Rack,* M-11462-OH-391-E (April 1991).

5. R. D. Dabbs et al., *HFIR Fuel-Storage Arrays (Multitier),* HFIR Design Change Memorandum, HFIR-169M (August 1994).

6. HFIR Drawing, *Jacket Assembly (Assembly),* M-11524-OH-011-E (November 1993).

7. J. A. Chapman, *Cadmium Verification Measurements of HFIR Shroud Assembly SA-22,* ORNL/TM-12718 (April 1994).

8. R. D. Dabbs, *HFIR Fuel-Storage-Array Criticality Safety Analysis (Single Tier),* C-HFIR-93-021/R0, HFIR Calculation (November 1991).

9. R. D. Dabbs, *Experimental Verification of Cadmium in Shroud Assembly 28,* HFIR Maintenance Work Package 31674 (November 1994)

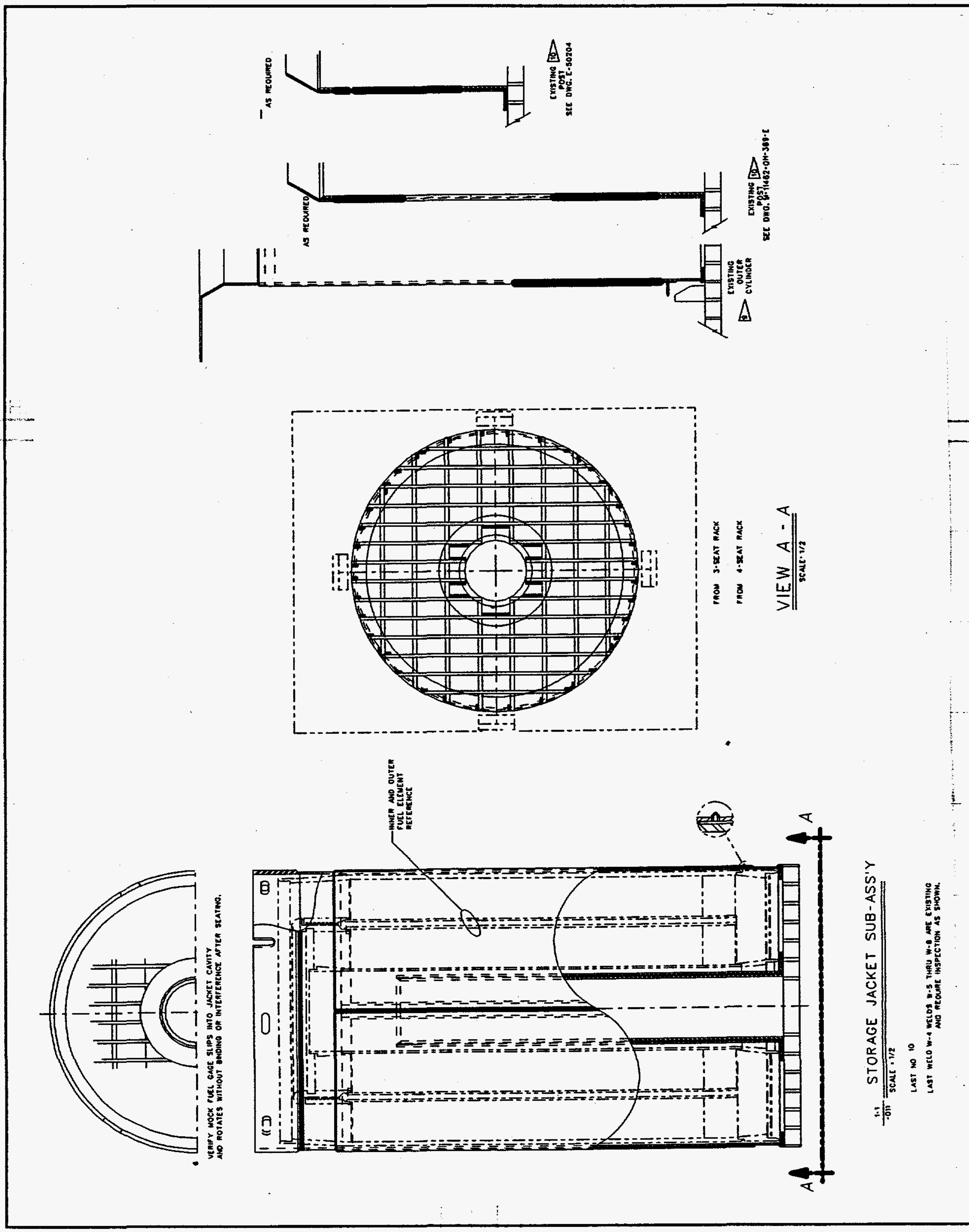

Figure 1. HFIR Shroud Assembly

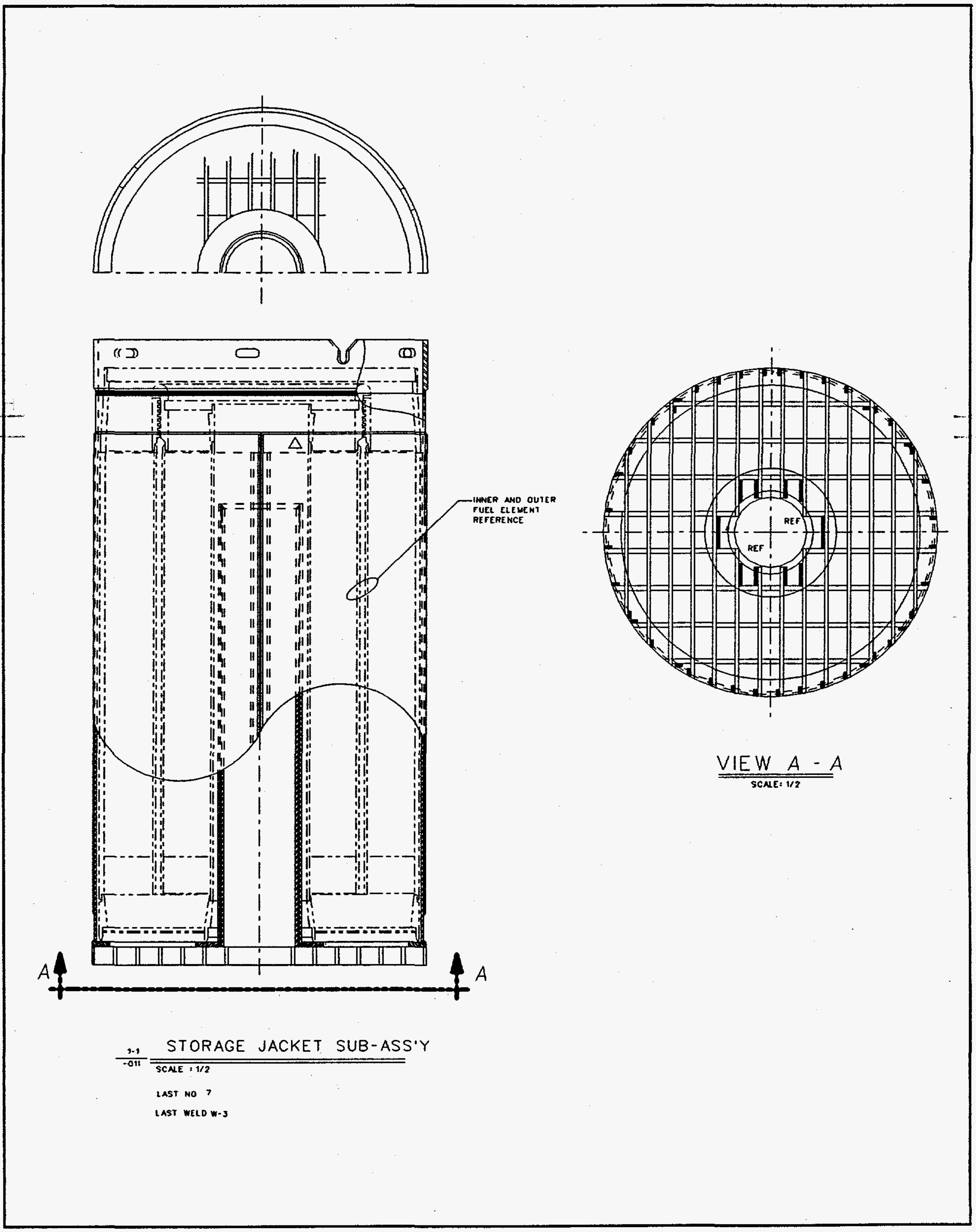

Figure 2. HFIR Jacket Assembly

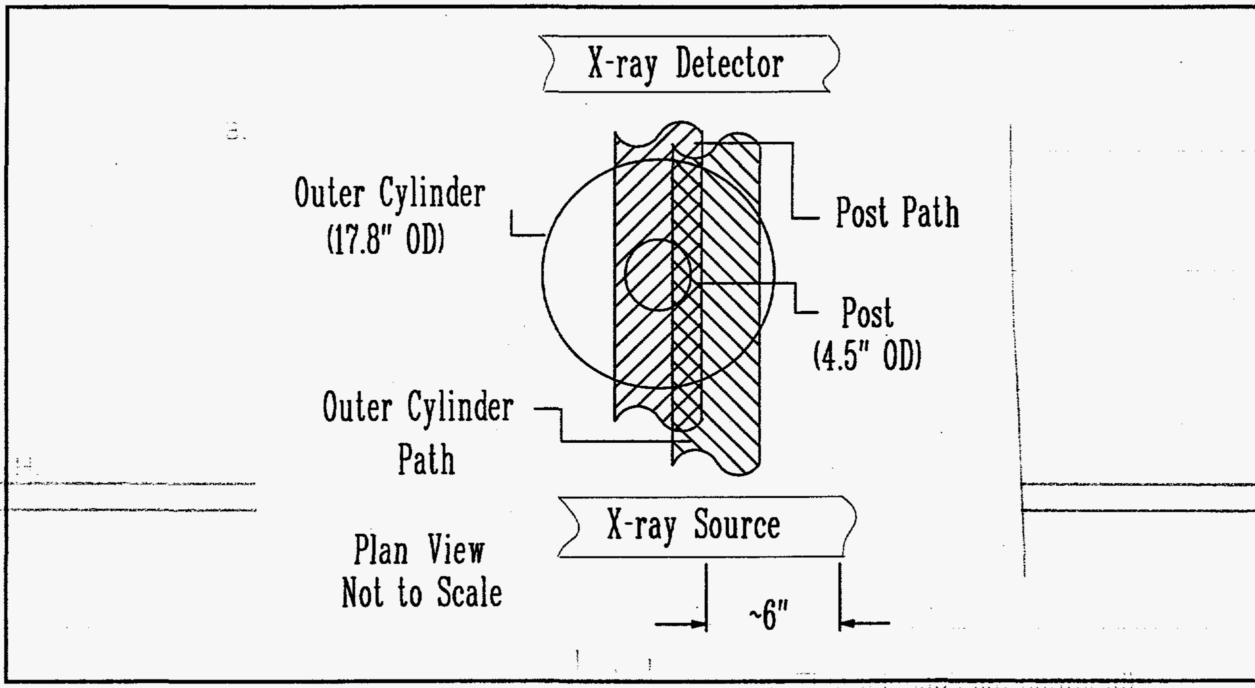

Figure 3. Thickness-Measurement Setup

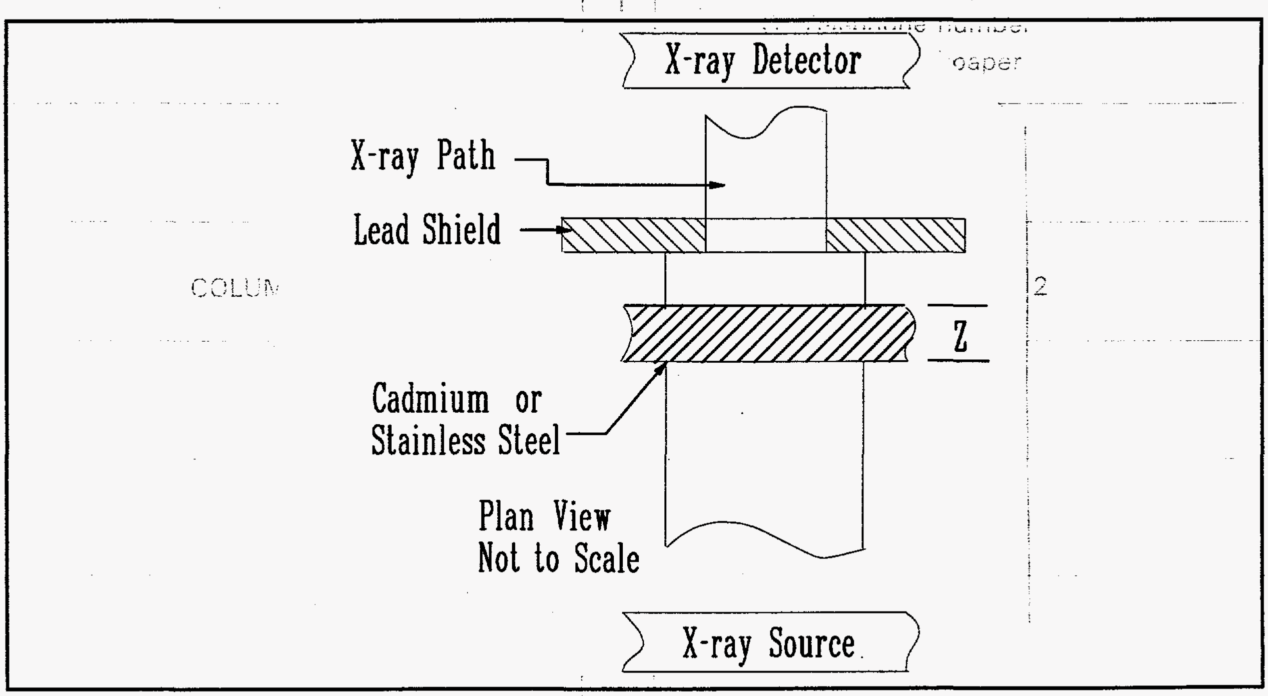

Figure 4. Attenuation-Coefficient Setup